

“Sighted C3H” mice – a tool for analysing the influence of vision on mouse behaviour?

Sabine M. Hoelter¹, Claudia Dalke¹, Magdalena Kallnik¹, Lore Becker^{2,5}, Marion Horsch², Anja Schrewe^{2,6}, Jack Favor³, Thomas Klopstock⁵, Johannes Beckers², Boris Ivandic⁶, Valérie Gailus-Durner², Helmut Fuchs², Martin Hrabé de Angelis², Jochen Graw¹, Wolfgang Wurst^{1,4}

¹Institute of Developmental Genetics, ²Institute of Experimental Genetics, ³Institute of Human Genetics, Helmholtz Center Munich - German Research Center for Environmental Health (GmbH), Ingolstaedter Landstraße 1, 85764 Neuherberg, Germany; ⁴Max-Planck-Institute of Psychiatry, Kraepelinstr. 2, 80804 Munich, Germany, ⁵Friedrich-Baur-Institute, Dept. of Neurology, University of Munich, Ziemssenstr. 1a, 80336 Munich, Germany, ⁶Dept. of Medicine III, University Heidelberg of Heidelberg, Im Neuenheimer Feld 410, 69120 Heidelberg, Germany

TABLE OF CONTENTS

1. Abstract
2. Introduction
3. Methods
3.1. Mice
3.2. Behavioural Phenotyping
3.2.1. Modified Hole Board (mHB)
3.2.2. SHIRPA
3.2.3. Pole Test
3.2.4. Lactate Levels
3.3. Eye Phenotyping
3.3.1. Funduscopy (Ophthalmoscopy)
3.3.2. Slit Lamp Biomicroscopy
3.3.3. Laser Interference Biometry (LIB)
3.3.4. Electroretinography
3.3.5. Optokinetic drum
3.3.6. Histology
3.4. Cardiovascular Phenotyping
3.4.1. Blood pressure
3.4.2. Surface limb ECG
3.4.3. Data analysis
3.5. Expression Profiling
3.5.1. Organ sampling & RNA isolation
3.5.2. cDNA microarrays
3.5.3. RNA labeling and hybridisation
3.5.4. Statistical analysis
3.5.5. BiblioSphere Pathway analysis
4. Results
4.1. Behavioural Phenotype
4.2. Eye Phenotype
4.3. Cardiovascular Phenotype
4.4. Expression Profiling
4.5. Functional Classification
5. Discussion
6. Acknowledgements
7. References

1. ABSTRACT

It is unclear what role vision plays in guiding mouse behaviour, since the mouse eye is of comparably low optical quality, and mice are considered to rely primarily on other senses. All C3H substrains are homozygous for the *Pde6b^{rd1}* mutation and get blind by weaning age. To study the impact of the *Pde6b^{rd1}* mutation on mouse behaviour and physiology, sighted C3H (C3H.Pde6b+) and normal C3H/HeH mice were phenotyped for different aspects. We confirmed *retinal degeneration 1* in C3H/HeH mice, and the presence of a morphologically normal retina as well as visual ability in

C3H.Pde6b+ mice. However, C3H.Pde6b+ mice showed an abnormal retinal function in the electroretinogram response, indicating that their vision was not normal as expected. C3H.Pde6b+ mice showed reduced latencies for several behaviours without any further alterations in these behaviours in comparison to C3H/HeH mice, suggesting that visual ability, although impaired, enables earlier usage of the behavioural repertoire in a novel environment, but does not lead to increased activity levels. These results emphasize the importance of comprehensive behavioural and physiological phenotyping.

2. INTRODUCTION

Behavioural phenotypes depend on multiple factors, amongst others on sensory inputs and on the processing of sensory information. Genetically diverse inbred mouse strains show a broad spectrum of phenotypes, some of them associated with known genetically determined physiological deficits (for review see (1)). The inbred mouse strain C3H is now among the most widely used of all mouse strains, e.g. it was used for at least one of several large-scale ENU (N-ethyl-N-nitrosourea) mutagenesis screens, in which several behavioural mutants have been found which are awaiting their detailed CNS function analysis (2-5). C3H mice are known to suffer from retinal degeneration due to inactivation of the rod photoreceptor cGMP phosphodiesterase 6 β -subunit (*Pde6b*) gene caused by a nonsense mutation and a retroviral insertion (6-8). Mice homozygous for the *Pde6b^{rdl}* mutation get blind by weaning age due to the rapid loss of rod photoreceptor cells through apoptosis and secondary degeneration of cones. *PDE6* is considered to be a protein specific to the retina (9).

Recently a congenic sighted C3H line devoid of retinal degeneration was introduced by Hart *et al.* (2005) (10). These mice were generated by crossing BALB/c with C3H/HeH and subsequent backcrossing of the *Pde6b* heterozygous offspring to C3H/HeH for 10 generations. Phenotypically normal heterozygotes were selected by fundus examination. Finally intercrossing these mice enabled selecting homozygotes for the wild-type *Pde6b* allele and these were used for subsequent breeding (10). Sighted C3H (C3H.*Pde6b*+) and normal C3H/HeH mice may be used to study the impact of vision on mouse behaviour. It is unclear what role vision plays in guiding mouse behaviour, since the mouse eye is of comparably low optical quality, and mice are believed to rely primarily on other senses (11). However, in 13 inbred strains with differing visual abilities, these have been shown to influence learning and memory in the Morris Water Maze as well as conditioned odor preference, but not motor learning performance (12). Interestingly, conditioned odor preference was enhanced in mice with visual defects, suggesting that visual abilities may not only influence the many behavioural tasks for rodents which depend on visual cues, but also tasks that rely on other sensory modalities (12).

To investigate the influence of intact *Pde6b* function on behaviour and physiology in the C3H strain, we compared the sighted C3H.*Pde6b*+/+ line and blind C3H/HeH control mice homozygous for the *Pde6b^{rdl}* allele in spontaneous behaviour, motor performance, eye phenotype, cardiovascular function and expression profiles of eye, brain and heart.

3. METHODS

3.1. Mice

Breeding pairs of sighted C3H (C3H.*Pde6b*+/+) and normal C3H/HeH mice were generated by Ian Jackson and Lisa McKie and obtained from MRC Harwell, UK (10). Offspring (n = 15 per genotype and sex) were bred in

the German Mouse Clinic (GMC) at the GSF, Germany, and run through the GMC primary screen (13). Genotypes were housed in different cages, but both genotypes were analysed concurrently. Results of screens with significant findings are reported.

3.2. Behavioural phenotyping

Behavioural phenotyping was carried out at the age of 9-10 weeks.

3.2.1. Modified Hole Board (mHB)

This test was carried out in our standard operating procedure as previously described (14, 15). This test allows the comprehensive analysis of a range of parameters known to be indicative of behavioural dimensions such as locomotor activity, exploratory behaviour, arousal, emotionality, memory and social affinity in a single short test (16). In brief, mice were allowed to explore a novel environment, while their cage mates were present in an adjacent group compartment, separated from the test arena by a transparent PVC partition with holes to allow group contact. A board with holes covered by motile lids was placed in the middle of the test arena, and for each trial, an unfamiliar object and a familiar object were placed into the test arena. At the beginning of an experiment, all animals of a cage were allowed to habituate together in the group compartment for 20 min. Then each animal was placed individually into the test arena and allowed to explore it freely for 5 min, during which the cage mates stayed present in the group compartment. During the 5 min trial, the animal's behaviour was recorded by a trained observer with a hand-held computer. Data were analyzed by using the Observer 4.1 Software (Noldus, Wageningen). Additionally, a camera was mounted 1.20 m above the center of the test arena, and the animal's track was videotaped and its locomotor path analyzed with a video-tracking system (Ethovision 2.3, Noldus, Wageningen). After each trial, the test arena was cleaned carefully with a disinfectant. Data were statistically analyzed using SPSS software (SPSS Inc, Chicago, USA). The chosen level of significance was $p < 0.05$.

3.2.2. SHIRPA

SHIRPA (Smithkline Beecham, MRC Harwell, Imperial College, the Royal London hospital Phenotype Assessment), Grip Strength and Accelerating Rotarod were assessed in our standard operating procedures as previously described (17). The Accelerating Rotarod procedure was used to measure fore limb and hind limb motor coordination, balance and motor learning ability (18). The mean latency to fall off the Rotarod during 3 trials was recorded and used in subsequent analysis. Before the start of the first trial, mice were weighed. For statistical analysis of the rotarod results linear mixed-effect models are fitted, that allow for the dependencies of genotype and trial and for the effects of sex and weight. The latter are modelled as fixed effects.

3.2.3. Pole test

This test was used for the assessment of motor coordination (19, 20). The device is made of a round, metal

“Sighted C3H” mice

threaded bar of 50 cm. This was inserted vertically in a platform. Each mouse was placed at the top of the bar with its head upwards. The style the mice climbed down the pole was categorized to allow for evaluation of motor performance. In addition the time the mice needed to reach the floor with all 4 paws was recorded. To decrease the effects of vision impairments a small plate with bedding from the home cage was placed at the bottom of the pole. All experimental equipment was thoroughly cleaned with Pursept-A and dried prior to testing. Values for body weight and pole time are presented as means \pm SEM and body weight was analyzed with 2-way-ANOVA. The Kruskal-Wallis-test (S-PLUS, Insightful) was used to test for effects of genotype and gender in the pole performance ratings. Pole time results are analyzed with an ANOVA analysis with weight as independent variable as well as genotype and sex.

3.2.4. Lactate levels

Plasma lactate levels were analyzed with an AU400 analyser. Blood lactate levels are a valid indicator for impaired energy metabolism. Organs with high energy demand like nervous tissue and muscle are sensitive to a lack of energy and various neurological phenotypes are associated with defects in energy supply.

3.3. Eye phenotyping

Unless indicated otherwise, eye phenotyping was carried out at the age of 11 weeks.

3.3.1. Funduscopy (Ophthalmoscopy)

The posterior parts of both eyes were examined after pupil dilation with one drop of atropine (1%). The mouse is grasped firmly in one hand and clinically evaluated using a head-worn indirect ophthalmoscope (Sigma 150 K, Heine Optotechnik, Herrsching, Germany) in conjunction with a condensing lens (90D lens, Volk, Fronhaeuser, Unterhaching, Germany) mounted between the ophthalmoscope and the eye. To take fundus photos the Heine Video Omega 2C Ophthalmoscope (Dieter Mann GmbH, Mainaschaff, Germany) was used in conjunction with a 40D lens (Volk, Fronhaeuser, Unterhaching, Germany).

3.3.2. Slit Lamp Biomicroscopy

Mice were examined biomicroscopically for anterior eye abnormalities as previously described (21). Briefly, pupils were dilated with a 1% atropine solution applied to the eyes at least 10 min prior to examination. Both eyes of the mice were examined by slit lamp biomicroscopy (Zeiss SLM30) at 48x magnification with a narrow beam slit lamp illumination at 25-30° angle from the direction of observation. Observed phenotypic variants of the eyes were carefully documented.

3.3.3. Laser Interference Biometry (LIB)

LIB was performed using the “ACMaster” (Meditec, Carl Zeiss, Jena, Germany) equipped with the new technique of optical low coherence interferometry (OLCI) as described by (22). Mice were anaesthetized with 137 mg Ketamine and 6.6 mg Xylazine per kg body weight and placed in front of the ACMaster. The mean value and

standard error was calculated and statistically analysed with the Student’s t-test using MS-Excel. Statistical significance was set at $p < 0.05$.

3.3.4. Electroretinography (ERG)

ERG was used to examine the retinal function as described (23). Scotopic ERGs were recorded from anaesthetized (137 mg/kg Ketamine and 6.6 mg/kg Xylazine) mice after at least 12 hours dark –adaptation and pupil dilation (1 % atropine) using an ESPION Ganzfeld stimulator and Console (Diagnosys LLC, Littleton, MA, USA) two steps at 500 and 12,500 cd/m².

3.3.5. Optokinetic drum

Vision tests were performed with an optokinetic drum setup (24), for details see Puk *et al.* in this issue. Briefly, the tested mouse was freely moving in a transparent acrylic glass cylinder which was placed in the center of the optokinetic drum, a rotating cylinder with a pattern of black and white stripes. Head-tracking reactions were analysed at a spatial frequency of 0.1 cyc/deg and a drum rotation speed of 10 rpm. The contrast was close to 100%.

3.3.6. Histology

Eyes were fixed 24 hours in Davidson solution, dehydrated and embedded in plastic medium (JB4-Plus, Polyscience, Inc., Eppelheim, Germany). Transverse 2 μ m sections were cut with an ultramicrotome (Ultratom OMU3, Reichert, Walldorf, Germany), stained with methylene blue and basic fuchsin and evaluated with a light microscope.

3.4. Cardiovascular phenotyping

Cardiovascular phenotyping was carried out at the age of 16 weeks.

3.4.1. Blood pressure

Blood pressure was measured in conscious mice with a non-invasive tail-cuff method using the MC4000 Blood Pressure Analysis Systems (Hatteras Instruments Inc., Cary, North Carolina, USA). Four animals were restrained on a pre-warmed metal platform in metal boxes. The tails were looped through a tail-cuff and fixed in a notch containing an optical path with a LED light and a photosensor. The blood pulse wave in the tail artery was detected by light extinction and transformed into a pulse amplitude signal. Pulse detection, cuff inflation and pressure evaluation were automated by the system software. After five initial inflation runs for habituation, 12 measurement runs were performed for each animal in one session. Runs with movement artefacts were excluded. After one day of training, in which the animals were habituated to the apparatus and protocol, the measurements were performed on four consecutive days between 8:30 and 11:30 AM.

3.4.2. Surface limb ECG

ECG was performed in anesthetized (isoflurane/pressured air inhalation) mice by use of three metal bracelets fixed at the joints of the feet covered with electrode gel. The complete setup was located in a faraday

“Sighted C3H” mice

cage. The electrodes were positioned on both front limbs and the left hind limb, resulting in the bipolar standard limb leads I, II and III and the augmented unipolar leads AVF, AVR, AVL. ECG was recorded for about seven minutes. A shape analysis of the ECG traces was performed with the software ECG-auto (EMKA technologies, Paris, France). For each animal, all standard ECG time intervals and amplitudes were evaluated from five different sets of averaged beats in lead II. The parameter QT interval was also corrected for the RR interval ($QT_c = QT / (RR/100)^{1/2}$) as recommended by Mitchell *et al.* (25). In addition, the recordings were screened for arrhythmias, including supraventricular and ventricular extrasystoles and conduction blockages.

3.4.3. Data analysis

For blood pressure analysis, at least 20 to 48 individual measurements were pooled to obtain a mean over the four measurement days for each animal. In the quantitative ECG analysis sets of five analyzed beats were averaged for one animal. The data were analyzed statistically using Statistica. Analysis of variance (ANOVA) tests are used for multi-factorial analysis of sex and genotype. Post hoc analysis for multiple comparisons is performed by Duncan's Multiple Range Test & Critical Ranges.

3.5. Expression profiling

3.5.1. Organ sampling & RNA isolation

Organs were archived of six male C3H.Pde6b+ and six control C3H/HeH mice at the age of 17 weeks for subsequent DNA chip expression profiling analysis. Eyes were collected of another 12 animals (6 C3H.Pde6b+ and 6 C3H/H3H) at the age of 8 weeks. To minimize the influence of circadian rhythm on gene expression mice were killed by carbon dioxide asphyxiation between 9-12 am. Organs were dissected, immediately frozen and stored in liquid nitrogen. Total RNA was isolated according to manufacturer's protocols (RNeasy Midi or Mini Kit; Qiagen). For the amplification of eye RNA of single animals according to the Target AMPTM 1-Round aRNA Amplification Kit 103 (Epicenter Biotechnologies, US) 400 ng total RNA was used.

3.5.2. cDNA microarrays

The glass cDNA-chip contains the fully sequenced 20K cDNA mouse array TAG library (Lion Bioscience, Heidelberg, Germany) and several hundred cDNA clones for genes that were not included in the commercial clone set. A full description of the probes on our microarray has been submitted to the GEO database (GPL4937) (26). In this database raw data of all analysed tissues are available (GSE7855). cDNA microarrays have been generated as recently described (27-30).

3.5.3. RNA labelling and hybridisation

Two independent dual colour hybridisations including a dye swap experiment were performed with RNA of single C3H.Pde6b+ organs. As reference a pool of C3H/HeH RNA of the same organ was used. For reverse transcription and labelling a modified TIGR protocol was used (27, 31). The procedure of pre-hybridisation,

hybridisation, washing and drying (nitrogen) was performed using a HS4800 Hybstation (Tecan, Männedorf, Switzerland). Dried slides were scanned with a GenePix 4000A microarray scanner and the images were analyzed with the GenePix Pro6.0 image processing software (Molecular Devices, CA, USA) (27, 30, 32).

3.5.4. Statistical analysis

Statistical analyses have been performed with TIGR Microarray Data Analysis System (TM4; (33, 34)). TM4 including MIDAS (Microarray Data Analysis System (35)) for normalization and SAM (Significant Analysis of Microarrays (33, 36)) for identification of genes with significant differential regulation were used. In SAM genes were ranked according to their relative difference value $d(i)$. Genes with $d(i)$ values greater than a set threshold (0.5) were selected as significantly differentially expressed. To estimate the False Discovery Rate (FDR), nonsense genes were identified by calculating 1000 permutations of the measurements. The FDR was lower than 10% in the datasets of the analysed organs.

3.5.5. BiblioSphere Pathway analysis

BiblioSphere Pathway Edition (Genomatix, Germany) was used to select pathways relevant for the selected genes. This software was used to filter significantly regulated genes for two categories of Gene Ontology (GO) terms: Biological Processes and Molecular Functions. A GO-Filter consists of a hierarchy of terms and the corresponding annotations for the BiblioSphere analysis. The z-score of the GO-terms indicates whether a certain annotation or group of annotations is over-represented in a dataset of genes (37).

4. RESULTS

4.1. Behavioural phenotype

Behavioural analysis of spontaneous activity in a novel environment, as measured by the modified Hole Board test, revealed a reduced latency to first line crossing in C3H.Pde6b+ mice compared to C3H/HeH controls (Table 1). C3H.Pde6b+ males exhibited reduced forward locomotor activity as measured by line crossing frequency, (Table 1), total distance travelled, turning frequency and mean velocity (Table 2). Concerning the path shape, C3H.Pde6b+ males made more changes in direction as evident from increased values for mean turn angle, angular velocity and absolute meander (Table 2). C3H.Pde6b+ females exhibited rearing behaviour significantly earlier and C3H.Pde6b+ mice of both sexes visited the board and started object exploration significantly earlier (Table 1). There was a trend in C3H.Pde6b+ males to approach the unfamiliar object less frequently than control males that just missed statistical significance, but they spent significantly less time exploring it (Table 1). C3H.Pde6b+ mice displayed more grooming behaviour and defecated more, but made less group contacts than controls. The time spent in social contact was significantly reduced in C3H.Pde6b+ females only (Table 1). There were no significant genotype effects on any other observed parameter.

Table 1. Results of behavioural observation in the modified Hole Board test

	Control		Mutant		Male + Female		ANOVA		
Parameter	Male (n=15)	Female (n=14)	Male (n=13)	Female (n=15)	Control (n=29)	Mutant (n=28)	sex	genotype	Interaction
Line crossing [frequency]	135 ± 6.7	84.5 ± 8.43	83.23 ± 4.83	84.73 ± 4.89	110.62 ± 7.09	84.04 ± 3.39	p<0.001	p<0.001	p<0.001
Line crossing [latency]	2.18 ± 0.73	3.55 ± 0.99	1.05 ± 0.22	1.86 ± 0.44	2.84 ± 0.61	1.49 ± 0.27	n.s.	p<0.05	n.s.
Rearings in box [frequency]	52.6 ± 3.38	26.21 ± 4.05	49.77 ± 4.65	35.53 ± 2.37	39.86 ± 3.58	42.14 ± 2.81	p<0.001	n.s.	n.s.
Rearings in box [latency]	26.96 ± 4.06	49.73 ± 7.12	24.18 ± 4.56	24.19 ± 3.33	37.95 ± 4.5	24.19 ± 2.72	p<0.05	p<0.01	p<0.05
Hole exploration [frequency]	63.2 ± 5.05	36.43 ± 7.7	46.54 ± 4.69	40 ± 3.58	50.28 ± 5.13	43.04 ± 2.92	p<0.01	n.s.	n.s.
Hole exploration [latency]	12.02 ± 3.61	55.36 ± 21.1	14.61 ± 4.85	24.59 ± 4.73	32.94 ± 10.95	19.95 ± 3.46	p<0.05	n.s.	n.s.
Hole visit [frequency]	0 ± 0	0 ± 0	0 ± 0	0 ± 0	0 ± 0	0 ± 0	n.s.	n.s.	n.s.
Hole visit [latency]	300 ± 0	300 ± 0	300 ± 0	300 ± 0	300 ± 0	300 ± 0	n.s.	n.s.	n.s.
Board entry [frequency]	7.87 ± 0.95	3.14 ± 0.77	5.77 ± 0.69	4.6 ± 0.82	5.59 ± 0.75	5.14 ± 0.54	p<0.001	n.s.	p < 0.05
Board entry [latency]	74.27 ± 9.36	168.14 ± 25.4	47.66 ± 5.24	77.02 ± 9.64	119.59 ± 15.68	63.39 ± 6.28	p<0.001	p<0.001	p < 0.05
Board entry [total duration %]	9.56 ± 1.29	4.58 ± 2.22	7.18 ± 1.46	6.95 ± 1.08	7.15 ± 1.33	7.06 ± 0.88	n.s.	n.s.	n.s.
Rearing on board [frequency]	2.6 ± 0.58	0.57 ± 0.2	1.62 ± 0.42	1.47 ± 0.42	1.62 ± 0.37	1.54 ± 0.29	p<0.05	n.s.	p<0.05
Rearing on board [latency]	173.07 ± 19.3	283.53 ± 6.66	196.09 ± 22.48	207.65 ± 23.08	226.4 ± 14.67	202.29 ± 15.92	p<0.01	n.s.	p<0.05
Risk assessment [frequency]	0.07 ± 0.07	0.57 ± 0.27	0 ± 0	0.2 ± 0.11	0.31 ± 0.14	0.11 ± 0.06	p<0.05	n.s.	n.s.
Risk assessment [latency]	281.13 ± 18.87	227.39 ± 32.08	300 ± 0	245.68 ± 29.06	255.19 ± 18.67	270.9 ± 16.18	p<0.05	n.s.	n.s.
Group contact [frequency]	14.73 ± 1.01	15.57 ± 1.78	11 ± 0.95	9.13 ± 0.93	15.14 ± 0.99	10 ± 0.67	n.s.	p<0.001	n.s.
Group contact [latency]	21.91 ± 3.81	45.26 ± 16.13	21.42 ± 3.23	23.58 ± 4.94	33.19 ± 8.18	22.58 ± 3	n.s.	n.s.	n.s.
Group contact [total duration %]	13.5 ± 1.59	16.76 ± 2.13	15.84 ± 1.51	10.34 ± 1.02	15.07 ± 1.33	12.89 ± 1.02	n.s.	n.s.	p<0.01
Grooming [frequency]	1.47 ± 0.56	1.07 ± 0.13	2.23 ± 0.58	2.6 ± 0.43	1.28 ± 0.29	2.43 ± 0.35	n.s.	p<0.05	n.s.
Grooming [latency]	201.16 ± 19.12	211.66 ± 13.22	144.86 ± 24.12	144.65 ± 15.35	206.23 ± 11.6	144.75 ± 13.62	n.s.	p<0.01	n.s.
Grooming [total duration %]	1.53 ± 0.55	1.44 ± 0.24	3.92 ± 1.12	2.72 ± 0.54	1.48 ± 0.3	3.28 ± 0.59	n.s.	p<0.01	n.s.
Defecation [frequency]	0.27 ± 0.15	0.86 ± 0.25	1.15 ± 0.44	1.27 ± 0.27	0.55 ± 0.15	1.21 ± 0.24	n.s.	p<0.05	n.s.
Defecation [latency]	275.95 ± 17.17	180.86 ± 35.17	234.45 ± 22.89	184.35 ± 30.23	230.04 ± 20.84	207.61 ± 19.62	p<0.01	n.s.	n.s.
Unfamiliar object exploration [frequency]	7.27 ± 0.86	4.79 ± 0.9	5.08 ± 0.7	6.2 ± 0.73	6.07 ± 0.65	5.68 ± 0.51	n.s.	n.s.	p<0.05
Familiar object exploration [frequency]	5.67 ± 0.8	4.5 ± 0.75	4.77 ± 0.56	6.47 ± 0.89	5.1 ± 0.55	5.68 ± 0.56	n.s.	n.s.	n.s.
Unfamiliar object exploration [latency]	32.02 ± 10.61	96.21 ± 24.43	28.8 ± 10.57	30.06 ± 17.03	63.01 ± 14.13	29.48 ± 10.18	n.s.	p<0.05	n.s.
Familiar object exploration [latency]	62.11 ± 19.26	72.86 ± 22.14	37.71 ± 10.37	37.12 ± 9.89	67.3 ± 14.38	37.39 ± 7.03	n.s.	p=0.07	n.s.
Unfamiliar object exploration [total duration %]	1.9 ± 0.28	1.29 ± 0.2	1.1 ± 0.1	1.65 ± 0.26	1.61 ± 0.18	1.39 ± 0.15	n.s.	n.s.	p<0.05
Familiar object exploration [total duration %]	1.15 ± 0.18	1.19 ± 0.22	0.98 ± 0.13	1.52 ± 0.24	1.17 ± 0.14	1.27 ± 0.15	n.s.	n.s.	n.s.
Object Index	0.22 ± 0.1	0.06 ± 0.15	0.07 ± 0.08	0.03 ± 0.1	0.14 ± 0.09	0.05 ± 0.06	n.s.	n.s.	n.s.

Data are presented as mean ± standard error of the mean.

All SHIRPA parameters were without significant findings (data not shown); only body weight was found to be reduced in C3H.Pde6b+ mice (Table 3). Plasma lactate levels were found to be reduced in C3H.Pde6b+ males (Table 4). Comparing the forelimb grip strength revealed no genotype-related differences (data not shown). We also checked motor coordination and balance with the accelerated rotarod. Mean values showed a big difference

with C3H.Pde6b+ mice performing much better resulting in longer latency time (Figure 1). The statistical analysis revealed a significant interaction of sex and weight effect (p<0.05), conveyable as a differing slope of the regression lines for weight and latency between sexes. In addition an interaction effect of sex and trial number (p<0.001) relates to different courses of improvement between sexes during ongoing trials. Subsequent analysis of sexes independently

“Sighted C3H” mice

Table 2. Video-tracking results of locomotor behaviour

Parameter	Control		Mutant		Male + Female		ANOVA		
	Male (n=15)	Female (n=14)	Male (n=14)	Female (n=15)	Control (n=29)	Mutant (n=29)	sex	genotype	Interaction
Total Distance Moved [cm]	3450.56 ± 146.54	2280.9 ± 186.93	2396.31 ± 122.87	2206.47 ± 128.61	2885.9 ± 159.96	2298.11 ± 89.34	p<0.001	p<0.001	p<0.01
Mean Velocity [cm/sec]	21.7 ± 0.65	16.63 ± 1.04	17.4 ± 0.58	16.96 ± 0.58	19.25 ± 0.76	17.17 ± 0.41	p<0.001	p<0.01	p<0.01
Maximum Velocity [cm/sec]	72.72 ± 3.19	66.89 ± 3.76	67.41 ± 3.19	67.29 ± 2.21	69.9 ± 2.47	67.34 ± 1.88	n.s.	n.s.	n.s.
Turns [Frequency]	1656.4 ± 46.48	1237.64 ± 68.31	1276.79 ± 45.85	1180.27 ± 48.75	1454.24 ± 56.29	1226.86 ± 34.19	p<0.001	p<0.001	p<0.01
Mean Turn Angle [degrees]	29.44 ± 0.73	35.06 ± 1.54	37.47 ± 1.02	33.63 ± 0.71	32.15 ± 0.97	35.49 ± 0.7	n.s.	p<0.01	p<0.001
Angular Velocity [degrees/sec.]	187.32 ± 3.62	194.52 ± 7.2	217.77 ± 5.45	193.22 ± 4.55	190.8 ± 3.93	205.07 ± 4.17	n.s.	p<0.01	p<0.01
Absolute Meander [degrees/sec.]	19.85 ± 0.58	24.46 ± 1.2	26.47 ± 0.86	23.64 ± 0.56	22.08 ± 0.77	25 ± 0.56	n.s.	p<0.001	p<0.001
Board entry [maximum duration. sec.]	10.13 ± 1.29	7.03 ± 3.64	9.46 ± 2.03	10.36 ± 1.55	8.64 ± 1.87	9.93 ± 1.25	n.s.	n.s.	n.s.
Mean distance to wall [cm]	7.27 ± 0.28	5.56 ± 0.64	6.61 ± 0.34	5.73 ± 0.27	6.45 ± 0.37	6.15 ± 0.23	p<0.01	n.s.	n.s.
Mean distance to board [cm]	8.55 ± 0.23	9.88 ± 0.56	9.23 ± 0.26	10.06 ± 0.21	9.19 ± 0.32	9.66 ± 0.18	p<0.01	n.s.	n.s.

Data are presented as mean ± standard error of the mean.

showed that weight is the major criterion for difference in performance. Weight effect was significant in males ($p<0.01$) and females ($p<0.05$) whereas strain effect was not significant in both sexes. Trial number had, as expected, significant influence (M: $p<0.05$, F: $p<0.01$). In the Pole test there was a slight reduction in time to descend the pole but only in males there was a significant difference in pole style between the two genotypes (Table 5).

4.2. Eye phenotype

Slit lamp biomicroscopy revealed no anterior segment abnormalities associated with the *Pde6b^{rd1}* allele. However, all C3H/HeH mice showed pigment patches and vessel attenuation in the retinal fundus, the characteristic abnormalities of *retinal degeneration 1*, associated with the *Pde6b^{rd1}* allele. No abnormalities were detected in the fundi of the C3H.Pde6b+ mice (Figure 2). The visual acuity of the mice was tested in the optokinetic drum. As expected, C3H/HeH mice showed no head-tracking reaction according to the moving stripes of the drum, while the C3H.Pde6b+ mice showed a response and scored at least once in 6 trials (Figure 3). In Laser Interference Biometry, the axial eye length of both eyes was determined. Since no differences were observed between the left and right eye (data not shown), data of both eyes were averaged for further evaluation (Table 6). No significant difference was observed for the body length of C3H/HeH and “sighted C3H” mice (Table 6). Sex-specific differences were observed only in the C3H.Pde6b+ group, after normalising the axial eye length with the body length. However, significant differences of the axial eye length were found, when comparing C3H.Pde6b+ (sighted) mice with the C3H/HeH controls (males and the females), attributed to the presence and absence of the photoreceptor cell layers in the retina. The histological analysis showed the characteristic loss of photoreceptor cells in C3H/HeH control mice, due to the *Pde6b^{rd1}* allele. C3H.Pde6b+ mice had a normal retina presenting all different layers (Figure 4).

ERG responses were recorded using a screening protocol with two different light intensities (23). As expected the control C3H/HeH mice showed no response to the flash light stimulus. Surprisingly, all tested C3H.Pde6b+ showed an abnormal ERG response without any b-wave response (Figure 5). No sex differences were observed. To confirm this result a different batch of 4 (2 males, 2 females) C3H.Pde6b+ mice was tested at the age of 6 weeks. The younger mice again showed an abnormal ERG response comparable to the first batch of mice tested. Different from C3H/HeH mice, in “sighted” C3H.Pde6b+ mice an a-wave is evoked at 12,500 cd/m². For comparison, the normal ERG response of a typical BALB/c mouse is added to Figure 4.

4.3. Cardiovascular phenotype

Blood pressure analysis did not reveal any genotype specific differences. ECG analysis (Table 7) revealed several genotype specific differences between mutant and control mice. C3H.Pde6b+ mice had a decreased PQ interval compared to the control C3H/HeH mice indicating differences within the atria or the specialized tissues of the conduction system. In addition, C3H.Pde6b+ mice showed a decreased QT interval and QTc, the QT interval corrected for heart rate. Within the QT interval, no difference was seen in the QRS complex duration but the ST interval was decreased in C3H.Pde6b+ mice., which suggests that the repolarization is more affected than the depolarization. A genotype effect was also seen in increased QRS amplitudes for both sexes together in the ANOVA, reaching the level of significance in the post hoc test only in males. Example ECG plots of a C3H/HeH and a C3H.Pde6b+ male are shown in Figure 6.

4.4. Expression profiling

Significantly regulated genes could be identified in eye, brain and heart. In eye, about 600 significantly regulated genes were found. These genes were reproducibly regulated in all experiments of six C3H.Pde6b+ mice. Due to the large amount of regulated genes our further study

“Sighted C3H” mice

Table 3. Recording of body weight

Parameter	Male			Female			both
	Control (n=15)	Mutant (n=15)	p-value	Control (n=15)	Mutant (n=15)	p-value	p-value
Body Weight [g]	32,9 ± 0,6	30,5 ± 0,5	<0,01	29,8 ± 0,6	25,7 ± 0,5	<0,001	<0,001

Data are presented as mean ± standard error of the mean

Table 4. Lactate levels

Parameter	Male			Female			both
	Control (n=15)	Mutant (n=15)	p-value	Control (n=15)	Mutant (n=15)	p-value	p-value
Lactate (mmo/l)	13,3 ± 0.2	11.6 ± 0.4	<0,001	11.2 ± 0,3	10.9 ± 0.3	n.s.	Interaction sex x strain <0,05

Data are presented as mean blood lactate concentrations ± standard error of the mean.

Table 5. Performance in the pole test

Parameter	Male			Female			both
	Control (n=15)	Mutant (n=15)	p-value	Control (n=15)	Mutant (n=15)	p-value	p-value
Stays over 30 sec.	0	0	<0,05	5	3	n.s.	<0,05
Falls	0	0		1	0		
Backwards	0	0		0	0		
Sideways	9	3		1	1		
Turns at bottom half	2	3		3	2		
Turns at top half	4	9	n.s.	5	9	n.s.	n.s.
Pole time (sec)	32.9 ± 4.0	26.0 ± 4.4		43.9 ± 3.5	41.0 ± 4.4		

Data are presented either in absolute numbers or as mean ± standard error of the mean (pole time).

concentrated on the top 200 regulated genes in eye. Several of these genes are associated with different retina diseases, corneal wound healing and apoptosis. Further, groups of regulated genes in the eye are expressed in corneal epithelium (*Aldh3a1*, *Anxa8*, *Aqp5*, *Cyp4b1*, *Klf4*, *Krt11-12*, *Krt1-19*, *Muc4*, *Prdx6* and *Tkt*) and different retina layers (*Cd31*, *Hbegf*, *RhoB*, *Rpgrip1*, *Sag* and *Unc119*).

In brain 10 genes were reproducibly differentially expressed on all microarray experiments of 6 C3H.Pde6b+ animals. The most interesting genes, *Gnas* and *Vdac1*, were both down-regulated in C3H.Pde6b+ mice. *Gnas* is a critical regulator of energy and glucose metabolism and a negative regulator of sympathetic nervous system activity in adult mice (38). Regulation of *Gnas* gave an indication for a higher sympathetic nervous system activity in C3H.Pde6b+ mice. Voltage-dependent anion channel (VDAC) proteins are small, abundant, pore-forming proteins and play an essential role in cellular metabolism and in early stages of apoptosis (39). *VDAC1* is involved in permeability transition pore (PTP) activity and/or regulation and thus an important player in retinal degeneration associated with PTP-mediated mitochondrial dysfunction (40).

Due to variability in expression patterns between the single mice in heart the selected genes were reproducibly regulated only in 4 out of 6 analysed mice. Inspection of expression data of heart from single mice revealed non-correlation of the expression patterns between the animals. Maybe biological variability in gene expression, oscillation or stress responsive genes were potential reasons for reduced correlation in the expression patterns between single individuals. In addition,

several recent publications have provided evidence for biological variability of expression levels for particular genes (29, 30, 41-44). Several of the significantly expressed genes in heart are involved in distinct heart failure. *Hdac9* and *Tcap* are associated with cardiac hypertrophy while *Csrp3* is a cardiomyopathy-associated gene (45-47). Overexpression of the inhibitor of apoptosis protein (*Iap*), playing an important role in both apoptosis and innate immunity (48), was detected in heart and brain.

4.5. Functional Classification

We analysed whether particular gene ontology terms (molecular functions or biological processes) were over-represented among the regulated genes in all three analysed organ types. For this we used the GO-Filter structure of the BiblospherePathway Edition. We considered a z-score >5.0 as indication for the over-representation of a certain annotation or group of annotations in a dataset of genes. In heart only one GO-term for biological processes (generation of precursor metabolites and energy) as well as for molecular functions (hydrogen ion transporter activity) was overrepresented (Table 8). For molecular functions in eye four terms were overrepresented which were annotated with structural constituent of cytoskeleton, glutathione transferase activity, tetrapyrrole binding and cytoskeletal protein binding (Table 8). Further, over-representation of five biological processes was observed in eye: regulation of muscles contraction, cytoskeleton organization and biogenesis, epidermis development, sensory perception of light stimulus and positive regulation of apoptosis (Table 8). Due to the low number of regulated genes in brain no over-represented GO-term was found.

“Sighted C3H” mice

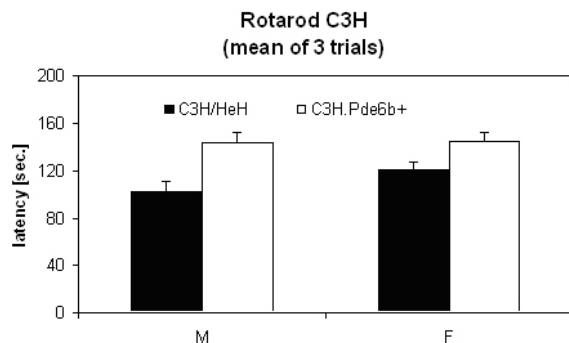


Figure 1. Results of Rotarod testing. C3H.Pde6b+ mice stayed significantly longer on the Rotarod than C3H/HeH mice.

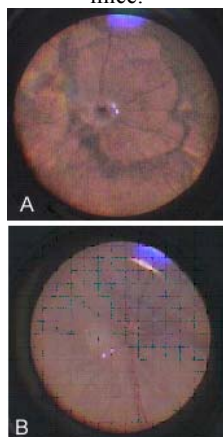


Figure 2. Fundus of C3H/HeH (A) and C3H.Pde6b+ (B) mice. A. C3H/HeH mice show the characteristic pigment patches and vessel attenuation, associated with the *Pde6b^{dl}* allele. B. C3H.Pde6b+ mice with a normal fundus appearance.

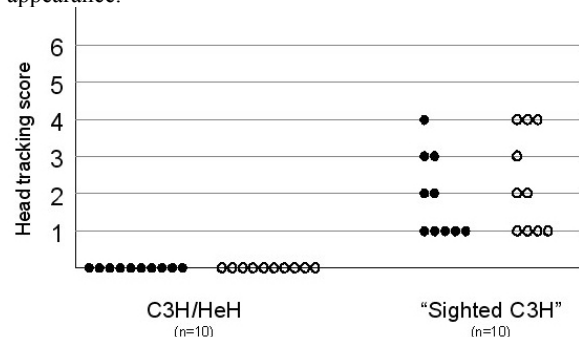


Figure 3. Head-tracking score distribution of C3H/HeH and “Sighted C3H” mice. Each spot represents the head-tracking score of one tested mouse obtained in the first (●) and second (○) vision test.

5. DISCUSSION

Analysis in the Eye Screen of the GMC confirmed the expected eye phenotype of C3H/HeH mice, related with the *Pde6b^{dl}* allele and the visual ability of sighted C3H.Pde6b+ mice. However, the number and intensity of responses to the moving stripes of the optokinetic drum

was lower than expected for normal sighted mice (Puk *et al.* this issue). Therefore a normal visual acuity of the C3H.Pde6b+ mice is doubtful. This was supported by the abnormal ERG response, indicating alterations in retinal function. The preserved a-wave response at 12,500 cd/m² pointed to intact photoreceptor function, while the missing b-wave suggested a malfunction of the retinal cells connected to the photoreceptors, mainly the bipolar cells.

Taking the C3H/HeH as reference for gene expression levels, expression of genes involved in apoptosis was reduced in C3H.Pde6b+ mice. *Bag3*, *Bnip1* and *Bzrp* are involved in apoptosis (49-51) and their up-regulation in eye may play a role in retinal degeneration (52). *Hbegf* showed reduced expression levels in C3H.Pde6b+ mice, a gene involved in wound-healing processes of the retina during proliferative retinopathies (53). The regulation of these genes might contribute to the degeneration of the retinal cells. In contrast, increased expression levels of genes associated with phototransduction or visual processes were identified in C3H.Pde6b+ mice. Expression of *Cds1*, *Rpgrip1*, *Sag* and *Unc119* in photoreceptor cells and their involvement in phototransduction was described (54-58). All four genes were up-regulated in the sighted C3H.Pde6b+ mice.

Custom retinal microarrays were developed to analyze differences in gene expression levels in retina of *rd1* (retinal degeneration 1) mutants (59). These studies resulted in about 200 regulated genes associated with photoreceptor cell death, apoptosis, neural remodeling, or more common retinal diseases. Association of regulated genes in our genome-wide expression studies with apoptosis and retinal diseases overlap with the studies of Hackam *et al.* (59). In contrast, we identified also genes regulated in corneal epithelium as well as genes involved in functions of the photoreceptor cells. These differences between the two studies may be caused by the different tissues (whole eye or retina) used for expression profiling analysis. Further, the analysis of Hackam *et al* focused on genes associated with retinal functions, while we performed un-biased genome-wide expression studies identifying 600 differentially regulated genes in the eyes.

The measurement of spontaneous behaviour in the modified Hole Board demonstrated a clear difference in C3H.Pde6b+ mice starting the exploration of the mHB earlier than C3H/HeH mice. The reduced latencies for several behaviours without any further alterations in these behaviours suggest that visual ability enabled earlier usage of the behavioural repertoire in a novel environment, but did not lead to generalised increased activity levels. Surprisingly, baseline values for forward locomotion were elevated in C3H/HeH males - the control group – both compared to C3H.Pde6b+ males and to female mice of both genotypes. From our experience with several batches of C3H mice from the C3HeB/FeJ sub-strain in this test we know that the average total distance travelled for C3H mice is about 2500 cm for both, male and female mice (unpublished observation). C3H/HeH females as well as C3H.Pde6b+ mice of both sexes analysed in this approach fit with on average 2300 cm to the C3HeB/FeJ sub-strain.

“Sighted C3H” mice

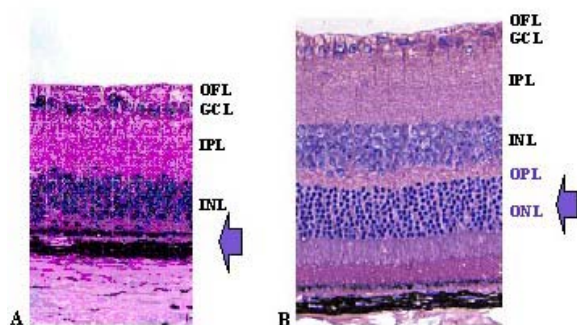


Figure 4. Histological analysis. A. C3H/HeH mice with the characteristic loss of photoreceptor cells. B. C3H.Pde6b+ mice with a normal retina. OFL – outer fiber layer, GCL – ganglion cell layer, IPL – inner plexiform layer, INL – inner nuclear layer, OPL – outer plexiform layer, ONL – outer nuclear layer.

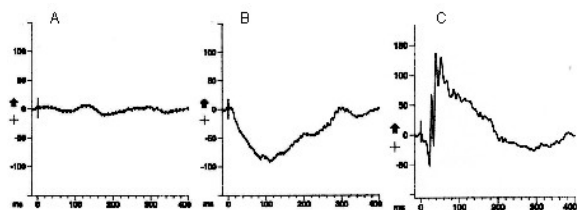


Figure 5. ERG responses. Typical responses of C3H/HeH (A) and C3H.Pde6b+ (B) recorded after a flash light stimulus of 12,500 cd/m². For comparison a normal ERG response of a BALB/c mouse is shown (C).

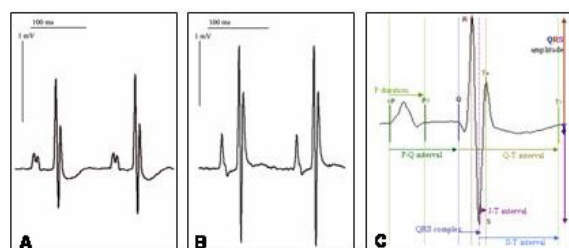


Figure 6. Electrocardiogram of lead II from anesthetized mice. Typical ECG of C3H/HeH (A) and Pde6b+ (B) males show the shorter PQ and QT, respectively ST intervals, and higher QRS amplitude in Pde6b+ mice. ECG parameters are indicated in an exemplified beat (C).

In contrast, with about 3400 cm of total distance travelled C3H/HeH males exhibited activity levels almost comparable to C57BL/6J mice with about 3600 cm in the mHB – and the B6 strain is a strain with a high baseline exploratory tendency (60).

Taking together the behavioural pattern of C3H.Pde6b+ mice in comparison to C3H/HeH, the “sighted” C3H.Pde6b+ mice were less cautious towards the exposed area (the board) since they entered it earlier, spent less time in group contact and exhibited increased grooming behaviour. Grooming behaviour in reaction to

novelty has an adaptive de-arousal function, and social contact during the test situation has been suggested to be more important for anxious animals than for less anxious ones (61, 62). Thus, the “sighted” C3H.Pde6b+ mice exhibited with their increased grooming-behaviour more active stress coping and consequently relied less on social contact during the test. Interestingly, this fits together with the expression profiling result of down-regulation of *Gnas*, a negative regulator of sympathetic nervous system activity, in C3H.Pde6b+ mice, suggesting an indication for a higher sympathetic nervous system activity in C3H.Pde6b+ mice.

This finding, in turn, fits together with the cardiovascular and the body weight phenotype. Prolongations of the different ECG intervals can appear due to alterations in the conduction properties of the heart. Comparing the C3H.Pde6b+ mice to the C3H/HeH control mice, the former present with higher values for the QRS amplitude. This difference was more pronounced in male mice. In humans alterations in the QRS amplitudes can reflect a change of the electrical axis of the heart. Increased amplitudes occur physiologically with a decreased vagal tone, which suggests increased sympathetic nervous system activity in C3H.Pde6b+ mice. Expression profiling data of the heart (tissue from male mice) show a striking differential regulation of genes concerning the respiratory chain or energy metabolism (e.g. *Cox7b*, *Cox4i1*, *Atp5b*, *Atp5o*, *Atp5f1*, *Hibch*, *Uqcrc2*). Comparing to the C3H/HeH controls, these genes were upregulated in the C3H.Pde6b+ mice. This finding is in line with decreased lactate levels in C3H.Pde6b+ mice, and may also be related to the body weight differences (C3H.Pde6b+ mice were lighter).

In conclusion, the surprising result of visual impairment in C3H.Pde6b+ mice indicates that this “sighted C3H” mouse line is not as good a tool to investigate the impact of vision on mouse behaviour as expected. The impaired retinal function observed in sighted C3H.Pde6b+ mice suggests a new mutation different from the *Pde6b* gene locus, which needs to be proven by crossings of C3H/HeH and C3H.Pde6b+ mice and evaluation of the offspring by ERG. If these crossings generate mice without visual impairment, these animals will be a better tool to address the role vision plays in guiding mouse behaviour. Even after 10 generations of backcrossing to C3H/HeH, a distinct region of about 20cM around the *Pde6b* gene that derives from BALB/c remains in the C3H.Pde6b+ mice. However, these BALB/c derived flanking regions can not be the reason for the retinal malfunction, because BALB/c mice have a normal ERG response (see Figure 5C). Likewise, most of the behavioural differences can not be explained by BALB/c flanking regions, since in the modified Hole Board BALB/c mice differ from C3H mice (own unpublished observations) in the amount of rearing and object exploration behaviour displayed, which did not differ between C3H/HeH and C3H.Pde6b+ mice, and by increased group contact, which was *reduced* in C3H.Pde6b+ mice. Whether the observed behavioural differences are solely due to the effect of *Pde6b* on vision

“Sighted C3H” mice

Table 6. Axial eye length

Parameter	Control (A)			Mutant (B)			A-B	A-B
	Male (n=15)	Female (n=15)	p - value	Male (n=15)	Female (n=15)	p - value	Male p - value	Female p - value
Axial length [mm]	3.526 ± 0.007	3.526 ± 0.008	n.s.	3.605 ± 0.004	3.609 ± 0.006	n.s.	<0.001	<0.001
body length [mm]	95.1 ± 0.502	93.9 ± 0.284	n.s.	95.6 ± 0.496	93.2 ± 0.571	<0.01	n.s.	n.s.
Axial length / body length	0.037 ± 0.0001	0.038 ± 0.0002	n.s.	0.038 ± 0.0002	0.039 ± 0.0002	<0.01	=0.02	<0.001

Data are presented as mean ± standard error of the mean, data of both eyes were averaged.

Table 7. Cardiovascular phenotype

Parameter	Control (A)		Mutant (B)		ANOVA			Post hoc test A~B	
	Male (n = 10)	Female (n = 10)	Male (n =10)	Female (n =10)	Sex p - value	Genotype p - value	Interact. p - value	Male p - value	Female p - value
PQ interval [ms]	34,4 +/- 0,5	36,0 +/- 0,8	32,1 +/- 0,6	33,0 +/- 0,2	p<0.05	p<0.001	n.s.	p<0.01	p<0.01
P-wave duration [ms]	20,3 +/- 0,6	19,7 +/- 0,5	18,8 +/- 0,3	20,1 +/- 0,5	n.s.	n.s.	n.s.	n.s.	n.s.
QRS-complex duration [ms]	9,8 +/- 0,3	8,9 +/- 0,2	9,3 +/- 0,2	8,8 +/- 0,3	p<0.01	n.s.	n.s.	n.s.	n.s.
QT interval [ms]	53,7 +/- 1,4	50,3 +/- 1,7	46,8 +/- 1,4	44,9 +/- 0,6	n.s.	p<0.001	n.s.	p<0.01	p<0.01
QT _{corrected} [ms]	46,6 +/- 0,9	43,9 +/- 1,5	40,3 +/- 0,9	39,2 +/- 0,8	n.s.	p<0.001	n.s.	p<0.001	p<0.01
RR interval [ms]	132,7 +/- 3,7	132,2 +/- 3,4	135,3 +/- 4,1	131,9 +/- 3,2	n.s.	n.s.	n.s.	n.s.	n.s.
Heart rate [bpm]	455,9 +/- 13,1	457,0 +/- 10,9	448,6 +/- 13,8	458,8 +/- 11,4	n.s.	n.s.	n.s.	n.s.	n.s.
JT interval [ms]	3,3 +/- 0,3	3,9 +/- 0,3	3,9 +/- 0,2	4,1 +/- 0,3	n.s.	n.s.	n.s.	n.s.	n.s.
ST interval [ms]	43,9 +/- 1,3	41,4 +/- 1,7	37,6 +/- 1,3	36,1 +/- 0,8	n.s.	p<0.001	n.s.	p<0.01	p<0.05
Q amplitude [mV]	0,01 +/- 0,00	0,01 +/- 0,00	0,02 +/- 0,00	0,02 +/- 0,00	n.s.	p<0.01	n.s.	n.s.	p<0.05
R amplitude [mV]	1,33 +/- 0,11	1,44 +/- 0,16	2,00 +/- 0,09	1,90 +/- 0,15	n.s.	p<0.001	n.s.	p<0.001	p<0.01
S amplitude [mV]	-0,29 +/- 0,07	-0,93 +/- 0,21	-0,91 +/- 0,18	-0,86 +/- 0,17	n.s.	n.s.	p<0.05	p<0.05	n.s.
QRS amplitude [mV]	1,62 +/- 0,12	2,40 +/- 0,18	2,92 +/- 0,16	2,75 +/- 0,18	n.s.	p<0.001	p<0.01	p<0.001	n.s.

Data are presented as mean ± standard error of the mean

Table 8. Gene Ontology

Organ	Function	GO-term	Gene symbols
Heart	Molecular functions	structural constituent of cytoskeleton	<i>Actr3, Actg1, Krt16, Tuba1b</i>
		structural constituent of ribosome	<i>Rpsa, Rpl14, Rpl4, Pps15, Uba52</i>
	Biological Processes	macromolecule biosynthetic process	<i>Rpsa, Rpl14, Rpl4, Rps15, Uba52</i>
Eye	Molecular functions	structural constituent of cytoskeleton	<i>Arbp, Cldn7, Krt1-12, Krt1-13, Krt1-14, Krt1-16, Krt1-19, Krt2-5, Lamc2, Nup155, Perq, Rpl11, Tnnc2, Tnni2, Tnni3, Tpm2, Unc119</i>
		glutathione transferase activity	<i>Gsta2, Gsta3, Gsta4, Gstt3</i>
		tetrapyrrole binding	<i>Alas2, Cyp2a5, Cyp2f2, Cyp4b1, Hba-x, Hbb-bhl</i>
		cytoskeletal protein binding	<i>Anxa2, Capg, Eps8l2, Flnc, Myh1, Nrap, Sdc1, Tmsb4x, Tnni2, Tpm2</i>
	Biological Processes	regulation of muscle contraction	<i>Atp2a1, Myh1, Myh8, Ryr1, Tnnc2, Tnni2, Tnni3, Tpm2</i>
		cytoskeleton organization and biogenesis	<i>Capg, Flnc, Krt1-12, Krt1-13, Krt1-14, Krt1-16, Krt1-19, Krt2-5, Myh1, Myh8, Nrap, Tmsb4x, Unc119</i>
		epidermis development	<i>Krt1-14, Krt2-5, Nif3, Sfn</i>
		sensory perception of light stimulus	<i>Guca1b, Rpgrip1, Sag, Unc199</i>
		positive regulation of apoptosis	<i>Aldh1a1, Bnpl1, Perq, Rarg, Scotin</i>

affected by its expression in the retina, or whether a so far unknown function of this gene in other tissues and organs contributes to the observed phenotypes remains to be

determined. Although PDE6b is considered to be an enzyme specific to the retina, mRNA for PDE6B has also been found in mouse hippocampus by RT-PCR, and a

hippocampal phenotype has been identified through a stereological study in C57BL/6J mice with the *rd/rd* genotype (9, 63, 64). Thus, it can not be excluded that *Pde6b* may also be expressed at very low levels in non-retinal tissues.

Taken together, the observation that C3H/HeH and C3H.Pde6b⁺ mice differed mainly in latencies to display several behaviours is best explained by their differences in visual abilities, and the unexpected finding of visual impairment in C3H.Pde6b⁺ mice stresses the importance of comprehensive phenotyping in mouse functional genomics.

6. ACKNOWLEDGEMENTS

We would like to thank Maria Kugler, Sandra Schaedler, Reinhard Seeliger and Cornelia Schneider for technical assistance, and Prof. Ian Jackson and Lisa McKie for producing the C3H.Pde6b⁺ line and helpful suggestions to the manuscript. We thank all the other members of the German Mouse Clinic for helpful discussions. This work has been funded by the Federal Ministry of Education and Research (BMBF) in the framework of the National Genome Research Network (NGFN), Foerderkennzeichen 01GR0448 and 01GR0430, and by the European Union (FP6, EUMODIC, LSHG-CT-2006-037188). The authors are responsible for the contents of this publication.

7. REFERENCES

1. J. N. Crawley, J. K. Belknap, A. Collins, J. C. Crabbe, W. Frankel, N. Henderson, R. J. Hitzemann, S. C. Maxson, L. L. Miner, A. J. Silva, J. M. Wehner, A. Wynshaw-Boris and R. Paylor: Behavioural phenotypes of inbred mouse strains: implications and recommendations for molecular studies. *Psychopharmacology (Berl)*, 132 (2), 107-24 (1997)
2. M. H. Hrabe de Angelis, H. Flaswinkel, H. Fuchs, B. Rathkolb, D. Soewarto, S. Marschall, S. Heffner, W. Pargent, K. Wuensch, M. Jung, A. Reis, T. Richter, F. Alessandrini, T. Jakob, E. Fuchs, H. Kolb, E. Kremmer, K. Schaeble, B. Rollinski, A. Roscher, C. Peters, T. Meitinger, T. Strom, T. Steckler, F. Holsboer, T. Klopstock, F. Gekeler, C. Schindewolf, T. Jung, K. Avraham, H. Behrendt, J. Ring, A. Zimmer, K. Schughart, K. Pfeffer, E. Wolf and R. Balling: Genome-wide, large-scale production of mutant mice by ENU mutagenesis. *Nat Genet*, 25 (4), 444-7 (2000)
3. D. Goldowitz, W. N. Frankel, J. S. Takahashi, M. Holtz-Vitaterna, C. Bult, W. A. Kibbe, J. Snoddy, Y. Li, S. Pretel, J. Yates and D. J. Swanson: Large-scale mutagenesis of the mouse to understand the genetic bases of nervous system structure and function. *Brain Res Mol Brain Res*, 132 (2), 105-15 (2004)
4. S. D. Brown and P. M. Nolan: Mouse mutagenesis-systematic studies of mammalian gene function. *Hum Mol Genet*, 7 (10), 1627-33 (1998)
5. U. H. Ehling, D. J. Charles, J. Favor, J. Graw, J. Kratochvilova, A. Neuhauser-Klaus and W. Pretsch: Induction of gene mutations in mice: the multiple endpoint approach. *Mutat Res*, 150 (1-2), 393-401 (1985)
6. R. L. Sidman and M. C. Green: Retinal Degeneration in the Mouse: Location of the Rd Locus in Linkage Group Xvii. *J Hered*, 56, 23-9 (1965)
7. S. J. Pittler and W. Baehr: Identification of a nonsense mutation in the rod photoreceptor cGMP phosphodiesterase beta-subunit gene of the rd mouse. *Proc Natl Acad Sci U S A*, 88 (19), 8322-6 (1991)
8. C. Bowes, T. Li, W. N. Frankel, M. Danciger, J. M. Coffin, M. L. Applebury and D. B. Farber: Localization of a retroviral element within the rd gene coding for the beta subunit of cGMP phosphodiesterase. *Proc Natl Acad Sci U S A*, 90 (7), 2955-9 (1993)
9. J. A. Beavo: Cyclic nucleotide phosphodiesterases: functional implications of multiple isoforms. *Physiol Rev*, 75 (4), 725-48 (1995)
10. W. Hart, L. McKie, J. E. Morgan, P. Gautier, K. West, I. J. Jackson and S. H. Cross: Genotype-phenotype correlation of mouse *pde6b* mutations. *Invest Ophthalmol Vis Sci*, 46 (9), 3443-50 (2005)
11. F. Schaeffel, E. Burkhardt, H. C. Howland and R. W. Williams: Measurement of refractive state and deprivation myopia in two strains of mice. *Optom Vis Sci*, 81 (2), 99-110 (2004)
12. R. E. Brown and A. A. Wong: The influence of visual ability on learning and memory performance in 13 strains of mice. *Learn Mem*, 14 (3), 134-44 (2007)
13. V. Gailus-Durner, H. Fuchs, L. Becker, I. Bolle, M. Brielmeier, J. Calzada-Wack, R. Elvert, N. Ehrhardt, C. Dalke, T. J. Franz, E. Grundner-Culemann, S. Hammelbacher, S. M. Holter, G. Holzwimmer, M. Horsch, A. Javaheri, S. V. Kalaydjiev, M. Klempt, E. Kling, S. Kunder, C. Lengger, T. Lisse, T. Mijalski, B. Naton, V. Pedersen, C. Prehn, G. Przemeck, I. Racz, C. Reinhard, P. Reitmeir, I. Schneider, A. Schrewe, R. Steinkamp, C. Zybill, J. Adamski, J. Beckers, H. Behrendt, J. Favor, J. Graw, G. Heldmaier, H. Hoffer, B. Ivandic, H. Katus, P. Kirchhof, M. Klingenspor, T. Klopstock, A. Lengeling, W. Muller, F. Oehl, M. Ollert, L. Quintanilla-Martinez, J. Schmidt, H. Schulz, E. Wolf, W. Wurst, A. Zimmer, D. H. Busch and M. H. de Angelis: Introducing the German Mouse Clinic: open access platform for standardized phenotyping. *Nat Methods*, 2 (6), 403-4 (2005)
14. F. Vauti, T. Goller, R. Beine, L. Becker, T. Klopstock, S. M. Holter, W. Wurst, H. Fuchs, V. Gailus-Durner, M. H. de Angelis and H. H. Arnold: The mouse *Trm1*-like gene is expressed in neural tissues and plays a role in motor coordination and exploratory behaviour. *Gene*, 389 (2), 174-85 (2007)

“Sighted C3H” mice

15. Bender, J. Beckers, I. Schneider, S. M. Holter, T. Haack, T. Ruthsatz, D. M. Vogt-Weisenhorn, L. Becker, J. Genius, D. Rujescu, M. Irmeler, T. Mijalski, M. Mader, L. Quintanilla-Martinez, H. Fuchs, V. Gailus-Durner, M. H. de Angelis, W. Wurst, J. Schmidt and T. Klopstock: Creatine improves health and survival of mice. *Neurobiol Aging* (2007)
16. F. Ohl, F. Holsboer and R. Landgraf: The modified hole board as a differential screen for behaviour in rodents. *Behav Res Methods Instrum Comput*, 33 (3), 392-7 (2001)
17. Schneider, W. S. Tirsch, T. Faus-Kessler, L. Becker, E. Kling, R. L. Busse, A. Bender, B. Feddersen, J. Tritschler, H. Fuchs, V. Gailus-Durner, K. H. Englmeier, M. H. de Angelis and T. Klopstock: Systematic, standardized and comprehensive neurological phenotyping of inbred mice strains in the German Mouse Clinic. *J Neurosci Methods*, 157 (1), 82-90 (2006)
18. B. J. Jones and D. J. Roberts: The quantitative measurement of motor inco-ordination in naive mice using an accelerating rotarod. *J Pharm Pharmacol*, 20 (4), 302-4 (1968)
19. S. Freitag, M. Schachner and F. Morellini: Behavioural alterations in mice deficient for the extracellular matrix glycoprotein tenascin-R. *Behav Brain Res*, 145 (1-2), 189-207 (2003)
20. T. Karl, R. Pabst and S. von Horsten: Behavioural phenotyping of mice in pharmacological and toxicological research. *Exp Toxicol Pathol*, 55 (1), 69-83 (2003)
21. Favor: A comparison of the dominant cataract and recessive specific-locus mutation rates induced by treatment of male mice with ethylnitrosourea. *Mutat Res*, 110 (2), 367-82 (1983)
22. O. Puk, C. Dalke, J. Favor, M. H. de Angelis and J. Graw: Variations of eye size parameters among different strains of mice. *Mamm Genome*, 17 (8), 851-7 (2006)
23. C. Dalke, J. Loster, H. Fuchs, V. Gailus-Durner, D. Soewarto, J. Favor, A. Neuhauser-Klaus, W. Pretsch, F. Gekeler, K. Shinoda, E. Zrenner, T. Meitinger, M. Hrabé de Angelis and J. Graw: Electroretinography as a screening method for mutations causing retinal dysfunction in mice. *Invest Ophthalmol Vis Sci*, 45 (2), 601-9 (2004)
24. C. Schmucker, M. Seeliger, P. Humphries, M. Biel and F. Schaeffel: Grating acuity at different luminances in wild-type mice and in mice lacking rod or cone function. *Invest Ophthalmol Vis Sci*, 46 (1), 398-407 (2005)
25. G. F. Mitchell, A. Jeron and G. Koren: Measurement of heart rate and Q-T interval in the conscious mouse. *Am J Physiol*, 274 (3 Pt 2), H747-51 (1998)
26. R. Edgar, M. Domrachev and A. E. Lash: Gene Expression Omnibus: NCBI gene expression and hybridization array data repository. *Nucleic Acids Res*, 30 (1), 207-10 (2002)
27. D. Greenwood, M. Horsch, A. Stengel, I. Vorberg, G. Lutzny, E. Maas, S. Schädler, V. Erfle, J. Beckers, H. Schatzl and C. Leib-Mosch: Cell line dependent RNA expression profiles of prion-infected mouse neuronal cells. *J Mol Biol*, 349 (3), 487-500 (2005)
28. Beckers, F. Herrmann, S. Rieger, A. L. Drobyshev, M. Horsch, M. Hrabé de Angelis and B. Seliger: Identification and validation of novel ERBB2 (HER2, NEU) targets including genes involved in angiogenesis. *Int J Cancer*, 114 (4), 590-7 (2005)
29. Drobyshev, M. Hrabé de Angelis and J. Beckers: Artefacts and reliability of DNA microarrays expression profiling data. *Current Genomics*, 4, 615-621 (2003)
30. Seltmann, M. Horsch, A. Drobyshev, Y. Chen, M. H. de Angelis and J. Beckers: Assessment of a systematic expression profiling approach in ENU-induced mouse mutant lines. *Mamm Genome*, 16 (1), 1-10 (2005)
31. P. Hegde, R. Qi, K. Abernathy, C. Gay, S. Dharap, R. Gaspard, J. E. Hughes, E. Snesrud, N. Lee and J. Quackenbush: A concise guide to cDNA microarray analysis. *Biotechniques*, 29 (3), 548-50, 552-4, 556 passim (2000)
32. M. Chinnaiyan, M. Huber-Lang, C. Kumar-Sinha, T. R. Barrette, S. Shankar-Sinha, V. J. Sarma, V. A. Padgaonkar and P. A. Ward: Molecular signatures of sepsis: multiorgan gene expression profiles of systemic inflammation. *Am J Pathol*, 159 (4), 1199-209 (2001)
33. V. G. Tusher, R. Tibshirani and G. Chu: Significance analysis of microarrays applied to the ionizing radiation response. *Proc Natl Acad Sci U S A*, 98 (9), 5116-21 (2001)
34. I. Saeed, V. Sharov, J. White, J. Li, W. Liang, N. Bhagabati, J. Braisted, M. Klapa, T. Currier, M. Thiagarajan, A. Sturn, M. Snuffin, A. Rezantsev, D. Popov, A. Ryltsov, E. Kostukovich, I. Borisovsky, Z. Liu, A. Vinsavich, V. Trush and J. Quackenbush: TM4: a free, open-source system for microarray data management and analysis. *Biotechniques*, 34 (2), 374-8 (2003)
35. J. Quackenbush: Microarray data normalization and transformation. *Nat Genet*, 32 Suppl, 496-501 (2002)
36. G. Chu, B. Narasimhan, R. Tibshirani and V. Tusher: SAM “Significance Analysis of Microarrays” Users Guide and Technical Document. <http://www-stat.standord.edu/~tibs/SAM/> (2002)
37. Scherf, A. Eppel and T. Werner: The next generation of literature analysis: integration of genomic analysis into text mining. *Brief Bioinform*, 6 (3), 287-97 (2005)
38. T. Xie, A. Plagge, O. Gavrilova, S. Pack, W. Jou, E. W. Lai, M. Frontera, G. Kelsey and L. S. Weinstein: The

“Sighted C3H” mice

alternative stimulatory G protein alpha-subunit XLalphas is a critical regulator of energy and glucose metabolism and sympathetic nerve activity in adult mice. *J Biol Chem*, 281 (28), 18989-99 (2006)

39. S. Liberatori, B. Canas, C. Tani, L. Bini, G. Buonocore, J. Godovac-Zimmermann, O. P. Mishra, M. Delivoria-Papadopoulos, R. Bracci and V. Pallini: Proteomic approach to the identification of voltage-dependent anion channel protein isoforms in guinea pig brain synaptosomes. *Proteomics*, 4 (5), 1335-40 (2004)

40. D. Gincel, N. Vardi and V. Shoshan-Barmatz: Retinal voltage-dependent anion channel: characterization and cellular localization. *Invest Ophthalmol Vis Sci*, 43 (7), 2097-104 (2002)

41. L. Drobyshchev, C. Machka, M. Horsch, M. Seltmann, V. Liebscher, M. Hrabe de Angelis and J. Beckers: Specificity assessment from fractionation experiments (SAFE): a novel method to evaluate microarray probe specificity based on hybridisation stringencies. *Nucleic Acids Res*, 31 (2), E1-1 (2003)

42. K. Oishi, K. Miyazaki, K. Kadota, R. Kikuno, T. Nagase, G. Atsumi, N. Ohkura, T. Azama, M. Mesaki, S. Yukimasa, H. Kobayashi, C. Iitaka, T. Umehara, M. Horikoshi, T. Kudo, Y. Shimizu, M. Yano, M. Monden, K. Machida, J. Matsuda, S. Horie, T. Todo and N. Ishida: Genome-wide expression analysis of mouse liver reveals CLOCK-regulated circadian output genes. *J Biol Chem*, 278 (42), 41519-27 (2003)

43. C. Pritchard, L. Hsu, J. Delrow and P. S. Nelson: Project normal: defining normal variance in mouse gene expression. *Proc Natl Acad Sci U S A*, 98 (23), 13266-71 (2001)

44. G. A. Churchill: Fundamentals of experimental design for cDNA microarrays. *Nat Genet*, 32 Suppl, 490-5 (2002)

45. Karamboulas, A. Swedani, C. Ward, A. S. Al-Madhoun, S. Wilton, S. Boisenue, A. G. Ridgeway and I. S. Skerjanc: HDAC activity regulates entry of mesoderm cells into the cardiac muscle lineage. *J Cell Sci*, 119 (Pt 20), 4305-14 (2006)

46. L. F. Tian, H. Y. Li, B. F. Jin, X. Pan, J. H. Man, P. J. Zhang, W. H. Li, B. Liang, H. Liu, J. Zhao, W. L. Gong, T. Zhou and X. M. Zhang: MDM2 interacts with and downregulates a sarcomeric protein, TCAP. *Biochem Biophys Res Commun*, 345 (1), 355-61 (2006)

47. J. M. Bos, R. N. Poley, M. Ny, D. J. Tester, X. Xu, M. Vatta, J. A. Towbin, B. J. Gersh, S. R. Ommen and M. J. Ackerman: Genotype-phenotype relationships involving hypertrophic cardiomyopathy-associated mutations in titin, muscle LIM protein, and telethonin. *Mol Genet Metab*, 88 (1), 78-85 (2006)

48. J. H. Leu, Y. C. Kuo, G. H. Kou and C. F. Lo: Molecular cloning and characterization of an inhibitor of

apoptosis protein (IAP) from the tiger shrimp, *Penaeus monodon*. *Dev Comp Immunol* (2007)

49. G. Jorda, A. Jimenez, E. Verdaguer, A. M. Canudas, J. Folch, F. X. Sureda, A. Camins and M. Pallas: Evidence in favour of a role for peripheral-type benzodiazepine receptor ligands in amplification of neuronal apoptosis. *Apoptosis*, 10 (1), 91-104 (2005)

50. G. Chiappetta, M. Ammirante, A. Basile, A. Rosati, M. Festa, M. Monaco, E. Vuttariello, R. Pasquinelli, C. Arra, M. Zerilli, M. Todaro, G. Stassi, L. Pezzullo, A. Gentilella, A. Tosco, M. Pascale, L. Marzullo, M. A. Belisario, M. C. Turco and A. Leone: The antiapoptotic protein BAG3 is expressed in thyroid carcinomas and modulates apoptosis mediated by tumor necrosis factor-related apoptosis-inducing ligand. *J Clin Endocrinol Metab*, 92 (3), 1159-63 (2007)

51. L. Shen, J. Hu, H. Lu, M. Wu, W. Qin, D. Wan, Y. Y. Li and J. Gu: The apoptosis-associated protein BNIP1 interacts with two cell proliferation-related proteins, MIF and GFER. *FEBS Lett*, 540 (1-3), 86-90 (2003)

52. Krizaj: Serca isoform expression in the mammalian retina. *Exp Eye Res*, 81 (6), 690-9 (2005)

53. Hollborn, I. Iandiev, M. Seifert, U. E. Schnurbusch, S. Wolf, P. Wiedemann, A. Bringmann and L. Kohen: Expression of HB-EGF by retinal pigment epithelial cells in vitreoretinal proliferative disease. *Curr Eye Res*, 31 (10), 863-74 (2006)

54. Y. Ishiba, T. Higashide, N. Mori, A. Kobayashi, S. Kubota, M. J. McLaren, H. Satoh, F. Wong and G. Inana: Targeted inactivation of synaptic HRG4 (UNC119) causes dysfunction in the distal photoreceptor and slow retinal degeneration, revealing a new function. *Exp Eye Res*, 84 (3), 473-85 (2007)

55. Mori, Y. Ishiba, S. Kubota, A. Kobayashi, T. Higashide, M. J. McLaren and G. Inana: Truncation mutation in HRG4 (UNC119) leads to mitochondrial ANT-1-mediated photoreceptor synaptic and retinal degeneration by apoptosis. *Invest Ophthalmol Vis Sci*, 47 (4), 1281-92 (2006)

56. M. Volta, A. Bulfone, C. Gattuso, E. Rossi, M. Mariani, G. G. Consalez, O. Zuffardi, A. Ballabio, S. Banfi and B. Franco: Identification and characterization of CDS2, a mammalian homolog of the *Drosophila* CDP-diacylglycerol synthase gene. *Genomics*, 55 (1), 68-77 (1999)

57. R. K. Koenekoop: RPGRIP1 is mutated in Leber congenital amaurosis: a mini-review. *Ophthalmic Genet*, 26 (4), 175-9 (2005)

58. K. Yamaki, M. Tsuda and T. Shinohara: The sequence of human retinal S-antigen reveals similarities with alpha-transducin. *FEBS Lett*, 234 (1), 39-43 (1988)

“Sighted C3H” mice

59. S. Hackam, R. Strom, D. Liu, J. Qian, C. Wang, D. Otteson, T. Gunatilaka, R. H. Farkas, I. Chowers, M. Kageyama, T. Leveillard, J. A. Sahel, P. A. Campochiaro, G. Parmigiani and D. J. Zack: Identification of gene expression changes associated with the progression of retinal degeneration in the rd1 mouse. *Invest Ophthalmol Vis Sci*, 45 (9), 2929-42 (2004)

60. J. N. Crawley and L. G. Davis: Baseline exploratory activity predicts anxiolytic responsiveness to diazepam in five mouse strains. *Brain Res Bull*, 8 (6), 609-12 (1982)

61. B. M. Spruijt, J. A. van Hooff and W. H. Gispen: Ethology and neurobiology of grooming behaviour. *Physiol Rev*, 72 (3), 825-52 (1992)

62. Ohl, N. Toschi, A. Wigger, M. S. Henniger and R. Landgraf: Dimensions of emotionality in a rat model of innate anxiety. *Behav Neurosci*, 115 (2), 429-36 (2001)

63. Z. Razzaque: Vascular reactivity in AB1-40 overexpressing double transgenic mice (APP695SWE x PS1A246E) and the interaction with the retinal degeneration (rd) PDE6 gene mutation. In: *8th International Conference on Alzheimer's Disease and Related Disorders*. Stockholm, Sweden (2002)

64. R. E. Wimer, C. C. Wimer, L. Alameddine and A. J. Cohen: The mouse gene retinal degeneration (rd) may reduce the number of neurons present in the adult hippocampal dentate gyrus. *Brain Res*, 547 (2), 275-8 (1991)

Key Words: C3H mice, *Pde6b*, Vision, Behaviour , Phenotyping

Send correspondence to: Dr. Sabine M. Höltér, Helmholtz Center Munich - German Research Center for Environmental Health, Ingolstädter Landstraße 1, 85764 Neuherberg, Germany, Tel: 498931873674, Fax: 498931873099, E-mail: hoelter@helmholtz-muenchen.de

<http://www.bioscience.org/current/vol13.htm>